

# Single-Molecule Approach to Enzymology

Sunney Xie

Harvard University  
Department of Chemistry and Chemical Biology  
12 Oxford Street, Cambridge, MA 02138, USA  
tel +617-496-9925  
fax +617-496-8709  
email xie@chemistry.harvard.edu

submitted 15 Aug 2001  
accepted 20 Nov 2001  
published 30 Nov 2001

## Abstract

Recent advances in single-molecule enzymology are reviewed. The theoretical underpinning of single-molecule enzymatic behaviors is discussed and exemplified by experiments and statistical analyses. In particular, the manifestations of the Michaelis-Menten mechanism, the kinetic scheme with sequential intermediates, and dynamic disorder in single molecule data are presented. A survey of current methods for single molecule enzymatic assays, especially those based on fluorescence detection, is presented as well.

## Introduction

It is fair to say, due to the efforts of many groups, that the single-molecule approach has changed the way biophysical or even biochemical problems are addressed. Many new insights derived from the approach are continuously emerging.

What new information is available from the single-molecule experiments? First, one can directly measure the distributions of molecular properties, rather than the ensemble average, by means of building a histogram of a particular variable for many molecules. This is straightforward conceptually, but tedious in practice. The distribution can arise either from static heterogeneity or dynamical fluctuations.

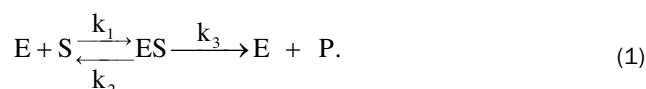
Second, and perhaps most important to biochemistry or chemical biology, is the ability of single-molecule experiments to follow biochemical processes in real time and capture transient intermediates, which previously could only be accomplished by synchronizing the actions of a large ensemble of molecules in order to create detectable concentrations of transient intermediates. This is particularly useful for elucidating reaction mechanisms. Perhaps one of the most beautiful examples is Kinosita and coworkers' direct observation of the discrete and stochastic  $120^\circ$  rotation steps of the  $\gamma$  subunit in  $F_1$ -ATPase [1], and their most recent observation that the  $120^\circ$  rotation step is composed of a  $90^\circ$  step and a  $30^\circ$  step, corresponding to the binding and hydrolysis of ATP, respectively [2]. Another example involves the capture of ribozyme folding intermediates by fluorescence resonant energy transfer [3].

Third, and perhaps least obvious, is that statistical analysis of single-molecule trajectories provides detailed dynamical information. Various methods of time series analysis can be applied to evaluate the trajectories, the results of which can be compared with physical models. The statistical analysis can uncover information in the stochastic trajectory that cannot be seen visually. This is where theoretical work is needed in order to facilitate the advancement of the field. I will touch on this subject below.

Meanwhile, techniques are still evolving, making possible the development of many new single-molecule assays, even in cellular environments. At the Spring School

for Optical Spectroscopy and Microscopy of Single Objects at Les Houches in France, organized by Orrit and colleagues, I gave lectures on our latest experiments using photo-induced electron transfer between flavin and tyrosine to probe conformational motion of single enzyme molecules at a broad span of time scales [4], as well as the new development in CARS microscopy aimed at a point-by-point chemical map of a live cell [5,6], and high resolution near-field microscopy aimed at spectroscopic imaging of biomembranes [7]. The readers are referred to the forthcoming references for details. Here I would like to give a general discussion of the principles of statistical analyses of enzymatic turnovers of single molecules and the practice of designing fluorescence assays of single-molecule enzymatic turnovers.

The fundamental reaction mechanism in enzymology, the Michaelis-Menten mechanism [8], is written as:



An enzyme (E) and a substrate (S) form a complex (ES) with a bimolecular rate constant  $k_1$ . The complex can either dissociate with a unimolecular rate constant  $k_2$  or form product with a unimolecular rate constant  $k_3$ . The kinetic equations for the Michaelis-Menten mechanism are

$$\frac{d[E]}{dt} = -k_1[E][S] + k_2[ES], \quad (2)$$

$$\frac{d[ES]}{dt} = k_1[E][S] - (k_2 + k_3)[ES], \quad (3)$$

$$\frac{d[P]}{dt} = k_3[ES]. \quad (4)$$

Conventional enzymatic assay on a large ensemble of molecules measures the enzymatic velocity

$$V = \frac{d[P]}{dt} = k_3[ES].$$

By invoking steady state approximation of [ES],

$$\frac{d[ES]}{dt} = k_1[E][S] - (k_2 + k_3)[ES] = 0, \quad (5)$$

and assuming the total enzyme concentration is  $[E_T] = [E] + [ES]$ , one obtains the celebrated Michaelis-Menten equation:

$$V = V_{\max} \frac{[S]}{[S] + K_m} \quad (6)$$

where  $V_{\max} = k_3[E_T]$  is the maximum enzymatic velocity at saturating substrate concentration, and  $K_m = (k_2 + k_3)/k_1$  is the substrate concentration at which the enzymatic rate is half of  $V_{\max}$ .  $V_{\max}$  and  $K_m$  can be determined by measuring  $V$  as a function of [S].

With ever increasing activities of single-molecule studies, it becomes important to think of chemical kinetics, in particular the Michaelis-Menten kinetics, on a single-molecule basis. In a single-molecule experiment, an enzyme molecule is immobilized by several means: (1) in agarose gel [9] or polyacrylamide gel [10]; (2) tethering onto the surface [1,3]; (3) trapped and manipulated by optical tweezers [11,12]; (4) tethered on a surface and manipulated by magnetic beads [13]. The dynamical variable can be the fluorescence intensity of the enzyme active site, as exemplified below, or the rotation angle of shaft of the  $F_1$ -ATPase[1], or the translational displacement of kinesin on a microtubule [11].

## Single-Molecule Enzymatic Reactions

Taking the cholesterol oxidase experiment as an example [9], the active site of the enzyme involves a tightly bound flavin adenine dinucleotide (FAD), which is naturally fluorescent in its oxidized form but not in its reduced form. Cholesterol is oxidized to cholesterone by the FAD via the Michaelis-Menten mechanism (Figure 1 inset).  $FADH_2$  in the enzyme is then oxidized by oxygen to regenerate FAD. As shown in Figure 1, fluorescence of a single enzyme molecule turns on and off as the FAD switches between the oxidized and reduced states, respectively. Each on-off cycle corresponds to an enzymatic turnover.

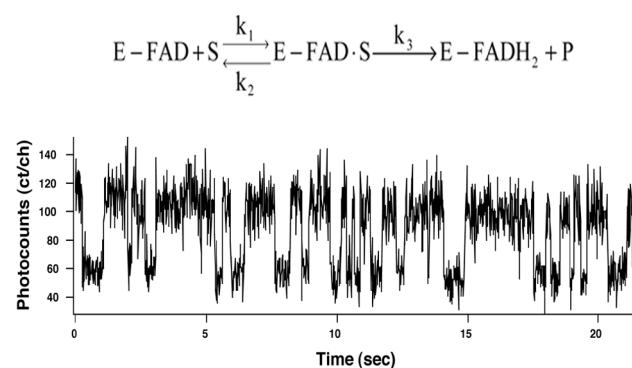
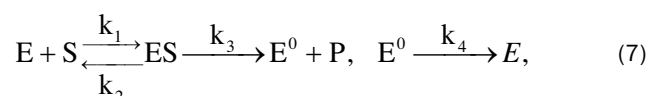


**Fig. 1.** Real-time observation of enzymatic turnovers of a single cholesterol oxidase (COx) molecule catalyzing oxidation of cholesterol molecules by oxygen. The emission from a single COx molecule as a function of time is plotted. Each on-off cycle in the emission intensity trajectory corresponds to an enzymatic turnover. The Michaelis-Menten mechanism of the enzymatic reaction is shown in the inset. Adapted from reference 9.

On a single molecule basis, the event of a chemical reaction, if it occurs, completes on the sub-picosecond time scale. We do not have sufficient time resolution in a single-molecule experiment to dissect such an action, but only to observe a sudden change in a dynamic variable. However, the waiting time prior to such a reaction is long on average. During this time, the molecule acquires sufficient energy to reach the transition state in a unimolecular reaction, or waits for combination with a diffusing substrate molecule in a bimolecular reaction. Such a waiting time is stochastic in nature, as shown in Figure 1. An individual event of a single-molecule reaction is not particularly informative. However, statistical properties of the trajectories, such as the distribution of waiting times, contain dynamical information, including the rates of the reactions.

Under conditions of single-molecule experiments, the concentration of an enzyme, however meaningless to define, has no bearing on the experimental observations. This does not implicate the breakdown of chemical kinetics, but rather necessitates a "single-molecule way of thinking" about chemical kinetics, i.e. to consider the probability rather than the concentration of the single enzyme molecule.

Let us now first find the probability distribution of the time it takes to complete an enzymatic reaction. To describe the cycling of an enzyme molecule, we modify Eq. 1 to



where  $E^0$  is the product of the first half reaction, which is reset back to  $E$  in the second half reaction. For example, in the cholesterol oxidase experiment,  $E$  (containing FAD) is reduced to  $E^0$  (containing FADH<sub>2</sub>) by cholesterol ( $S$ ) in the first half reaction, and  $E^0$  is converted back to  $E$  by oxygen in the second half reaction, which is known as the Ping-Pong mechanism [8].

Let's consider only the first half reaction. The concentrations of  $E$ ,  $ES$  and  $E^0$  in Eq. 2-4 are replaced by the probabilities for finding the enzyme molecule in the three states at time  $t$ :

$$\frac{dP_E(t)}{dt} = -k_1 P_E(t) + k_2 P_{ES}(t), \quad (8)$$

$$\frac{dP_{ES}(t)}{dt} = k_1 P_E(t) - (k_2 + k_3) P_{ES}(t), \quad (9)$$

$$\frac{dP_{E^0}(t)}{dt} = k_3 P_{ES}(t). \quad (10)$$

It is important to note that  $k_1^0 = k_1 [S]$  is the pseudo-first-order rate constant, proportional to  $[S]$ . The relationship  $k_1^0 = k_1 [S]$  holds whether  $[S]$  is high or low. In contrast, in ensemble experiments, a pseudo-first-order rate cannot be used when  $[S]$  is comparable to or lower than  $[E]$ .

The initial conditions for solving the coupled differential equations Eq. 8-10 are

$$P_E(0) = 1, P_{ES}(0) = 0, P_{E^0}(0) = 0, \quad (11)$$

with  $t = 0$  being the onset of an enzymatic reaction and  $P_E(t) + P_{ES}(t) + P_{E^0}(t) = 1$ .

We can then evaluate the probability density,  $f(\tau)$ , with  $\tau$  being the time required to complete the first half reaction. The probability for finding a particular  $t$  is  $f(\tau) \Delta\tau$ , which is equal to the probability of switching from the  $ES$  state to the  $E_0$  state between  $t=\tau$  and  $\tau + \Delta\tau$ ,  $\Delta P_{E^0}(t) = k_3 P_{ES}(t) \Delta\tau$ , or

$$f(\tau) = \left. \frac{dP_{E^0}(t)}{dt} \right|_{t=\tau} = k_3 P_{ES}(\tau). \quad (12)$$

Solving Eq. 8-10 for  $P_{ES}(t)$  by Laplace transform with the initial conditions Eq. 11 yields

$$f(\tau) = \frac{k_1^0 k_3}{2a} \{ \exp[(a+b)\tau] - \exp[(b-a)\tau] \}, \quad (13)$$

Where

$$a = \sqrt{\frac{1}{4} (k_1^0 + k_2 + k_3)^2 - k_1^0 k_3}, \quad b = -\frac{1}{2} (k_1^0 + k_2 + k_3).$$

$f(\tau)$  has an exponential rise followed by an exponential decay. This expression was given in reference [9].

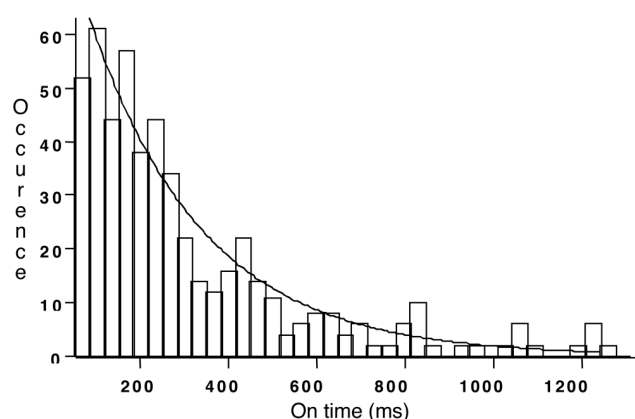


**Fig. 2.** Histogram of the on-times of a COx intensity trajectory taken at a high substrate concentration (2 mM) at which  $k_3$  is rate-limiting. The solid line is a single exponential fit with  $k_2 = 3.9 \pm 0.5 \text{ s}^{-1}$ . Adapted from reference 9.

Returning to our specific example in Figure 1, emission on-times refer to the times for the first half reaction to take place. The probability density  $f(\tau)$  is experimentally measured by the histogram of emission on-times (Figure 2 and Figure 3), providing the information regarding  $k_1^0$ ,  $k_2$ ,  $k_3$ . Similarly, the histogram of emission off-times provides the information about the second half reaction [9].

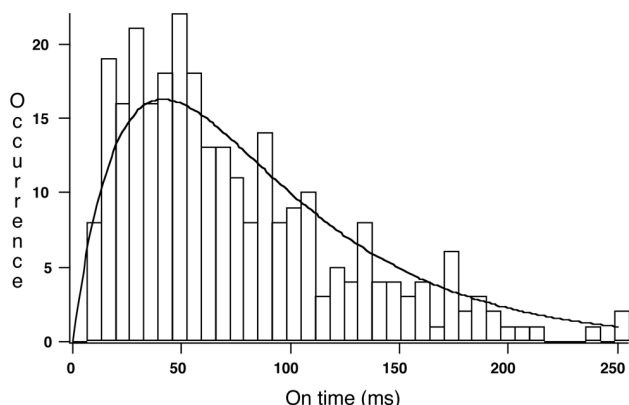


**Fig. 3.** Histogram of the on-times of a COx intensity trajectory when  $k_3$  is not rate-limiting. The solid line is the convolution of two exponentials (Eq. 14) with time constants  $k_1 = 33\text{s}^{-1}$  and  $k_3 = 17\text{s}^{-1}$ ,  $k_2 = 0$ . Adapted from ref. 9.

Such on and off histograms have been extensively used in the ion-channel literature [14]. In the single  $F_1$ -ATPase [1] and the myosin [15] experiments, the dwell times between consecutive steps are measured. Under the condition that resetting E from  $E^0$  is fast ( $k_4 \gg k_3$ ), the histogram of the dwell times reflects  $f(\tau)$  of the rate limiting step(s). The discussion here also holds for nonenzymatic reactions that have neither repetitive turnovers nor continuous trajectories. The folding of a single ribozyme initiated by flowing  $\text{Mg}^{2+}$  ions through the system is an example [3]. The histogram of the time required for the reaction can be constructed from events of many individual molecules, provided that static heterogeneity among the molecules is negligible.

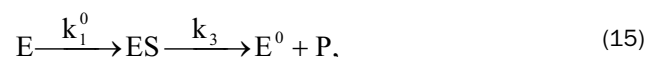
Let us now consider a few limiting cases of Eq. 13. When the  $k_3$  is rate limiting, the waiting time distribution is a single exponential function,  $f(\tau) = k_3 \exp(-k_3 \tau)$ , with the decay rate of  $k_3$  being the maximum turnover rate. This is what one would expect for a Poisson process [14]. Figure 2 shows such a situation. Similarly, when the substrate binding becomes rate limiting at low substrate concentrations,  $f(\tau)$  is approximately a single exponential distribution with a time constant of  $1/k_1^0$ .

Another limiting case is when the dissociation rate of the ES complex is negligible,  $k_2 = 0$ , Eq. 13 becomes

$$f(\tau) = \frac{k_1^0 k_3}{k_3 - k_1^0} [\exp(-k_1^0 \tau) - \exp(-k_3 \tau)] \quad (14)$$

which has an exponential rise of the faster of  $k_1^0$  and  $k_3$ , followed by an exponential decay of the slower the two rates. This is the situation in Figure 3.

Eq. 14 can be obtained in a different way by considering the kinetic scheme involving two sequential steps [16]:



If the time interval for the first step is  $\tau'$ , then the time interval for the second step is  $\tau - \tau'$ .

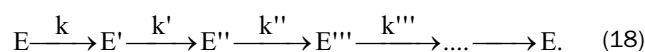
$$f(\tau) = \int_0^\tau f_1(\tau') f_2(\tau - \tau') d\tau' \quad (16)$$

is the convolution of two exponential functions,  $f_1(\tau') = k_1^0 \exp(-k_1^0 \tau')$  and  $f_2(\tau - \tau') = k_3 \exp[-k_3(\tau - \tau')]$ . Taking Laplace transform of Eq. 16,

$$\hat{f}(s) = \hat{f}_1(s) \hat{f}_2(s) = \frac{k_1^0}{(s + k_1^0)} \frac{k_3}{(s + k_3)}. \quad (17)$$

The inverse Laplace transform of  $\hat{f}(s)$  results in Eq. 14.

The shape of  $f(\tau)$  reveals mechanistic information. If there is only one rate limiting step,  $f(\tau)$  is exponential. A  $f(\tau)$  with an exponential rise and exponential decay indicates the existence of a Michaelis-Menten complex (for either zero or nonzero  $k_2$ ). In reality, the reaction may have more than one intermediate,



If the rates,  $k, k', \dots$  are comparable, i.e. there are several rate limiting steps, the distribution of  $\tau$  becomes narrower than that of one intermediate case. The distribution provides the information about the number of intermediates or rate limiting steps, even though the intermediate cannot be observed directly.

Assuming that there are  $n$  rate limiting intermediates and that the rates of the sequential steps are the same ( $k$ ), the dwell time distribution is

$$f(\tau) = \frac{k^n \tau^{n-1} e^{-k\tau}}{(n-1)!} \quad (19)$$

which is the convolution of  $n$  exponential functions  $p_0(\tau) = k \exp(-k\tau)$ , obtained by the inverse Laplace transform of  $\hat{f}(s) = \hat{f}_0^n(s)$ ,  $\hat{f}_0(s) = k/(s+k)$  [14].

In the limit of large  $n$ ,  $f(\tau)$  becomes a Gaussian distribution,

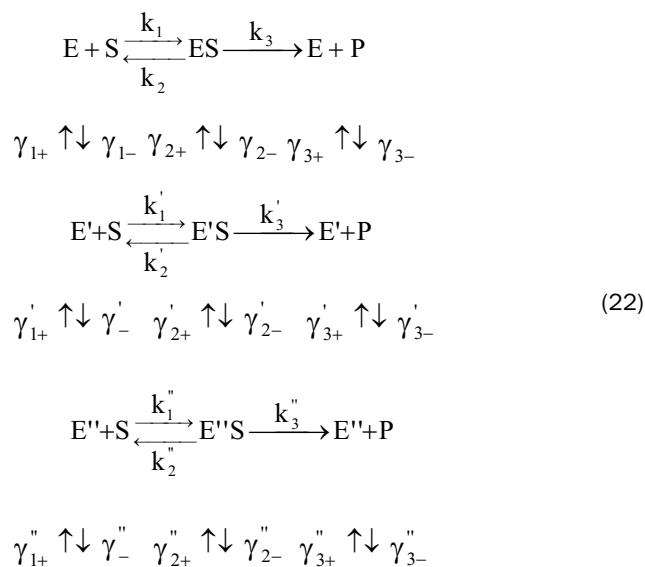
$$f(\tau) \approx \frac{k}{\sqrt{2\pi n}} \exp\left[-\frac{(r - n/k)^2}{2n/k^2}\right] \text{ for large } n \quad (20)$$

which is a consequence of the central limit theorem. When  $n$  approaches infinity, the relative width of  $f(\tau)$ ,  $\frac{\sqrt{n}/k}{n/k}$ , is approaching zero. This is why a cellular or physiological response involving many intermediates occurs within a deterministic rather than stochastic time interval. For trajectories with a limited number of turnovers, and thus limited statistics, it is helpful to evaluate the width of the distribution using the randomness parameter,

$$r = \frac{\langle \tau^2 \rangle - \langle \tau \rangle^2}{\langle \tau \rangle^2}, \quad (21)$$

without knowing  $f(\tau)$ . This method was introduced by Block and coworkers [16]. For a one-step Poisson process,  $f(\tau) = k \exp(-k\tau)$ ,  $\langle \tau \rangle = 1/k$ ,  $\langle \tau^2 \rangle - \langle \tau \rangle^2 = 1/k^2$ , therefore,  $r = 1$ . In general,  $0 < r < 1$ . Assuming similar rates in  $n$  rate-limiting steps, the variance of  $\tau$  on the numerator of Eq. 21 is  $n/k^2$ , while the denominator is  $n^2/k^2$ . Therefore,  $r \sim 1/n$ . The more rate limiting steps there are, the smaller the  $r$  is.  $r$  is zero for infinite  $n$ . In practice,  $r$  gives the low limit of the number of rate limiting steps. It was used to determine how many ATP molecules are needed for an 8-nm step of kinesin [16, 11].

So far we have only considered the sequential mechanisms in Eq. 1 and Eq. 18. Consider what would happen for a "parallel" reaction mechanism as follows:



$E$ ,  $E'$  and  $E''$  can be viewed as different conformations of the enzyme with interconverting rates,  $\gamma_x$ , among them. Experimentally, we often do not have an observable to distinguish them, except that they have different enzymatic rates. This means, on a single-molecule basis, that the

enzymatic rate fluctuates with time. This general phenomenon is called dynamic disorder [18].

Let's consider what happens to the distribution  $f(\tau)$ . In the case that  $k_3$  (or  $k_1$ ) is rate limiting, if the interconversion rates,  $\gamma_x$ , are faster than  $k_3$  (or  $k_1$ ),  $f(\tau)$  should be single exponential with the decay constant being the average of the limiting rates for all conformers,  $\langle k_x \rangle$ . If  $\gamma_x < k_x$ ,  $f(\tau)$  a multiexponential (instead of single exponential) distribution of  $p(\tau)$ . In fact, in the ion channel literature, multiexponential histograms of channel opening times were reported and attributed to conformational fluctuation [19]. For single-molecule enzymatic assays, the histograms of dwell times usually do not have good enough statistics to distinguish single or multiexponential distributions. In addition, the distribution is a scrambled histogram, in which interconversion rates ( $\gamma_x$ ) are not reflected. What we need is a way to evaluate how a dwell time is affected by its previous dwell times.

A sensitive way to evaluate the dynamic disorder is the autocorrelation function of the dwell times,

$$C(m) = \frac{\langle \Delta\tau(0) \Delta\tau(m) \rangle}{\langle \Delta\tau \rangle^2} = \frac{\sum_i \Delta\tau(i) \Delta\tau(i+m)}{\sum_i \Delta\tau^2(i)}, \quad (23)$$

where  $m$  is the index number for the turnovers and  $\Delta\tau(m) = \tau(m) - \langle \tau \rangle$ , with the bracket denoting the average along the trajectory. The physical meaning of  $C(m)$  is as follows: In the absence of dynamic disorder,  $C(0) = 1$  and  $C(m) = 0$  ( $m > 0$ ). This holds for not only a one step Poisson process ( $k_1$  or  $k_3$  rate limiting), but also the multiple intermediate case (Eq. 18). In the presence of dynamic disorder,  $C(m)$  has a decay, with the initial ( $m = 1$ ) amplitude reflecting the variance of the rate among different conformations and the decay time yielding the time-scale of the interconversion.

Figure 4 shows the  $C(m)$  derived from a single-molecule trajectory of cholesterol oxidase with saturating substrate. The decay constant is  $1.0 \pm 0.3$  s. Dynamic disorder of  $k_3$  is evident. In contrast, at low substrate concentration,  $C(m)$  has a spike only at zero time, indicating the absence of dynamic disorder of  $k_1$ . This experiment indicates that the enzyme has at least two metastable conformations with different  $k_3$ . The variation of the rate is rather large, an order of magnitude difference when assuming two conformers in order to account for the  $C(m)$  [18]. Our recent experiments indicated that there are more than just two conformers, but rather a distribution of them [4].

This fluctuation of the reaction rate ( $k_3$ ), which is a non-Markovian behavior (a memory effect), is the consequence of ignoring the details of the conformations ( $E, E', E'' \dots$ ) and grouping them into the species ( $E, ES, E^o$ ) in the Michaelis-Menten scheme (Eq. 1). When more details about the conformations are known (e.g. Eq. 22), each kinetics step is Markovian with a constant rather than fluctuating rate.

Single-molecule studies of dynamic disorder have been the subject of increasing numbers of theoretical work [20-24].

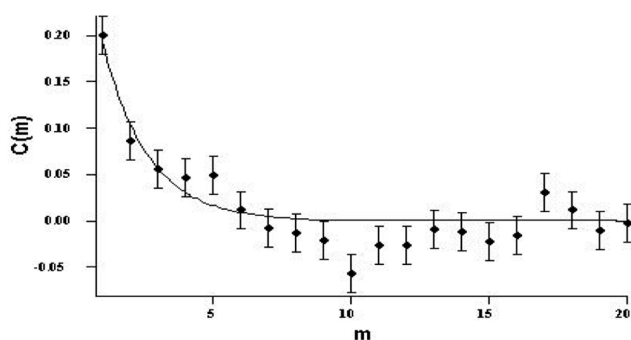


**Fig. 4.** Autocorrelation function of the on-times for a COx trajectory at saturating substrate concentration.  $C(m) =$

$$\frac{\langle \Delta\tau(0) \Delta\tau(m) \rangle}{\langle \Delta\tau^2 \rangle} = \frac{\sum_i \Delta\tau(i) \Delta\tau(i+m)}{\sum_i \Delta\tau(i)}, \text{ and}$$

$m$  being the index numbers of turnovers.  $\Delta\tau(m) = \tau(m) - \langle \tau \rangle$ . The fact that  $C(m)$  is not simply a spike at  $m = 0$  indicates dynamic disorder of  $k_3$ . The time constant of the decay gives the time-scale of the  $k_3$  fluctuation. Adapted from reference 9.

Of particular interest are methods for unveiling the hidden information regarding conformational states and their chemical activities. We do not yet understand the microscopic details of the conformations, except that the barrier heights between the states are relatively high ( $\sim 16$  kcal/mole assuming an Arrhenius process with a prefactor of  $10^{12}\text{s}^{-1}$ ), comparable to breaking and reforming a few hydrogen bonds. The structure fluctuations influencing the reaction rate can be either global changes of the entire protein or local changes at the active site.

We expect the dynamic disorder to be a general phenomenon in enzymology, which has been often masked in ensemble-averaged measurements. Similar slow rate changes have been inferred previously from other monomeric enzyme systems, and hypothesized to be relevant to physiological enzymatic regulation [25]. The physiological relevance of the dynamic disorder phenomenon, if any, will be best investigated by single-molecule experiments in cellular environments.

In the past few years, more and more single-molecule assays have been developed. No different from enzymology in general, single-molecule enzymology is primarily limited by the development of assays. Most of the successful assays involve processive enzymes associated with molecular motors. Fluorescent assays are still limited. Here I would like to give an assessment of current methods for single-molecule enzymatic assays based on fluorescence detection, with the hope of stimulating more assay development.

## Fluorescent Substrate

The time for a small substrate molecule to diffuse in and out of a diffraction-limited volume in aqueous solution is about  $10 \mu\text{s}$ – $1\text{ms}$ . If a fluorescent substrate can bind an enzyme molecule for a longer time, it can be detected. Yanagida and coworkers reported the use of fluorescent ATP derivative to monitor the ATP hydrolysis on a single myosin molecule [26]. The problem with this type of assay is that the substrate concentration has to be kept very low ( $\sim \text{nM}$ ) in order to suppress the background fluorescence. Therefore the turnover rate is diffusion limited. Total internal reflection microscopy is preferred for this type of assay because of its small excitation volume.

## Fluorescent Active Site

The cholesterol oxidase experiment given above is an example of this type of assay. The problem with the assay is that photobleaching limits the length of trajectories. For reasons we do not fully understand, cholesterol oxidase protects the flavin so that it actually emits more photons than dye molecules.

## Fluorescent Product

Rigler and co-workers reported an assay of horseradish peroxidase, which catalyzes the oxidation of the reduced form of rhodamine to the fluorescent rhodamine by hydrogen peroxide [27]. Many enzymatic reactions are limited by product release. The up-holding of the fluorescent product by the enzyme allows the detection of turnover events. The advantage of this type of assay is that photobleaching is not a problem, because the fluorescent product molecules are continuously produced and diffuse away from the excitation volume.

## Fluorescence Resonant Energy Transfer (FRET) Probe

Weiss and coworkers reported an assay for staphylococcal nuclease using a FRET pair consisting of fluorescent labels in the protein [28]. Enzymatic turnovers are monitored by their synchronous conformational changes. Careful design of specific labeling of the FRET pair is needed for this type of assay. One needs to make sure that the endogenous dyes do not interfere with the enzymatic reactions. Photobleaching of the labels often limits the length of the trajectory. Though little understanding of the photochemistry associated with photobleaching of dye molecules is available, readers are referred to a review article by Seidel et al on reduction of photobleaching [29].

## Photo-induced Electron Transfer Probe

We have recently used photo-induced electron transfer between excited states of flavin and tyrosine residues to

probe conformational motions associated with enzymatic reactions of flavoenzymes [4]. Complementary to FRET, electron transfer probes conformational changes occurring at a shorter distance (several Å) than FRET probes (several nm). The electron transfer rate (fluorescence quenching rate) is proportional to  $\exp(-\beta x)$ ,  $x$  being the edge-to-edge between the donor and the acceptor, and  $\beta \sim 0.7-1.5 \text{ \AA}^{-1}$ . The electron transfer probes can be composed of a limited number of naturally occurring amino acids or cofactors.

## Rotation Trajectory

Kinosita and coworkers' experiment on F1-ATPase tracked the rotation trajectories of the  $\gamma$  subunit, the shaft of the rotary motor. Although single fluorescence labels may be used to track the rotation, particularly with polarization sensitive detection, photobleaching limits the photon counts. For this reason, a fluorescent actin fiber [1] or a gold particle [2] was used. The strong signal of the latter allowed the use of a high-speed camera to capture the transient intermediates with a high time resolution. Another example is the direct observation of the relative rotation of RNA polymerase and RNA by using a magnetic and fluorescent bead [30].

## Translational Trajectory

Translational trajectory of possessive motor enzymes such kinesin [11], myosin [15], RNA polymerase [31,32], DNA polymerase [12, 33] and helicase [34] can be tracked by a CCD camera. Without high spatial and temporal resolutions needed to resolve individual enzymatic turnovers, one can already extract much useful information from these assays. When individual enzymatic turnovers need to be resolved, the center position of a diffraction-limited spot can be accurately determined within a couple of nanometers given enough signal averaging. For example, the 8-nm steps of a kinesin molecule can be resolved by viewing a tethered bead and signal averaging the Brownian motion trajectory at a low ATP concentration [35], or by tracking the bead with optical tweezers with better accuracy [11]. The manipulation by optical tweezers [11,12] or magnetic beads [33] allows studying enzymatic reactions under constant and controlled force loads. The mechanical manipulation in combination with fluorescence measurements [26] can be particularly informative. Many good assays have been developed using optical tweezers and magnetic beads on motor proteins. I have, for the most part, limited the discussion to fluorescence work here.

Fluorescence assays on a single-molecule basis, though prone to photobleaching, offer versatility, structure sensitivity and arguably a higher time resolution. No doubt more and more single-molecule assays will be developed. Some may even be easier than ensemble assays. I hope

that the material summarized above will be useful to the ever-increasing single-molecule studies.

*Acknowledgment:* I thank former and current members of my group, particularly Peter Lu, Haw Yang, Antoine van Oijen, Guobin Luo, and Long Cai for helpful discussions, and DOE and NIH for funding our effort on single-molecule enzymology.

## References

- [1] R. Yasuda, H. Noji, K. Kinosita, M. Yoshida, *Cell*, **93**, 1117 (1998).
- [2] R. Yasuda, H. Noji, M. Yoshida, K. Kinoshita, H. Itoh, *Nature*, **410**, 898, (2001).
- [3] X. Zhuang, L. E. Bartley, H. P. Babcock, R. Russell, T. Ha, D. Herschlag, S. Chu, *Science*, **288**, 2048 (2000).
- [4] Y. Haw, P. Karnchanaphanurach, X.S. Xie, to be published.
- [5] J. Cheng, A. Volkmer, L.D. Book, X.S.Xie, *J. Phys. Chem. B* **105**: 1277 (2001).
- [6] A. Volkmer, J. Cheng and X. S. Xie, *Phys. Rev. Lett.* **87**: 023901 (2001).
- [7] E.J. Sanchez, L. Novotny, X.S. Xie, *Phys. Rev. Lett.* **82**, 4014 (1999).
- [8] T. Palmer, *Understanding Enzymes* ed. 4, Prentic-Hall, New York, 1991.
- [9] H.P. Lu, L. Xun, X.S. Xie, *Science*, **282**, 1877-1882 (1998).
- [10] R. M. Dickson, A. B. Cubitt, R. Y. Tsien, W. E. Moerner, *Nature*, **388**, 355 (1997).
- [11] M. S. Schnitzer, S.M. Block, *Nature*, **388**, 386, (1997).
- [12] G.J.L. Wuite, S.B. Smith, M. Young, D. Keller, C. Bustamante, *Nature*, **404**, 103 (2000).
- [13] T. Strick, J.F. Allemand, V. Croquette, D. Bensimon, *Progress in Biophysics & Molecular Biology*, **74**, 115, (2000)
- [14] D. Colquham and A. G. Hawkes in *Single-Channel Recording*, 2nd ed., B. Sakmann, E. Neher, eds. Plenum Press, New York, 1995. pp 397-46
- [15] M. Rief, R.S. Rock, A.D. Mehta, M.S. Mooseker, R.E. Cheney, J.A. Spudich, *PNAS*, **97**, 9482 (2000).
- [16] M. J. Schnitzer, S. M. Block, *Cold Spring Harbor Symp. Quant. Biol.* 60 (Protein Kinesis: The Dynamics of Protein Trafficking and Stability), **793** (1995).
- [17] R. Zwanzig, *Acc. Chem. Res.* **23**, 148 (1990).
- [18] K. Rubinson, *Biophysical J.* **61**, 463 (1992).
- [19] J. Wang and P. Wolynes, *Phys. Rev. Lett.* **74**, 4317 (1995).
- [20] G. K. Schenter, H. P. Lu, X. S. Xie, *J. Phys. Chem. A* **103**, 10477 (1999).
- [21] J. Cao, *Chem. Phys. Lett.*, **327**, 38 (2000).

- [23] N. Agmon, *J. Phys. Chem. B*, **104**, 7830 (2000).
- [24] G. H. Weiss, J. Masoliver, *Physica A (Amsterdam, Neth.)* **296**, 75 (2001).
- [25] C. Frieden, *Ann. Rev. Biochem.* **48**, 471 (1979).
- [26] T. Funatsu, Y. Harada, M. Tokunaga, K. Saito, T. Yanagida, *Nature*, **374**, 555 (1995).
- [27] L. Edman, Z. Foldes-Papp, S. Wennmalm, R. Rigler, *Chem. Phys.* **247**, 11 (1999).
- [28] T. Ha, A.Y. Ting, J. Liang, W.B. Caldwell, A.A. Deniz, D. Chemla, P.S. Schultz, S. Weiss, *PNAS*, **96**, 893 (1999).
- [29] C. Eggeling, J. Widengren, R. Rigler, C.A.M. Seidel, in *Applied Fluorescence in Chemistry, Biology and Medicine* Eds: W. Rettig, B. Strehmel, S. Schrader, H. Seifert, p. 193, Springer-Verlag Berlin (1998).
- [30] Y. Harada, O. Ohara, A. Takatsuki, H. Itoh, N. Shimamoto, K. Kinoshita. *Nature*, **409**, 113 (2001).
- [31] M. Wang, M. J. Schnitzer, H. Yin, R. Landick, J. Gelles, S. M. Block, *Science*, **282**, 902 (1998).
- [32] H. Yin, I. Artsimovitch, R. Landick, J. Gelles, *PNAS*, **96**, 13124 (1999).
- [33] B. Maier, D. Bensimon, V. Croquette, *PNAS*, **97**, 12002 (2000).
- [34] K. M. Dohoney, J. Gelles *Nature*, **409**, 370 (2001).
- [35] W. Hua, E. C. Young, M.L. Fleming, J. Gelles, *Nature*, **390**, 390 (1997).